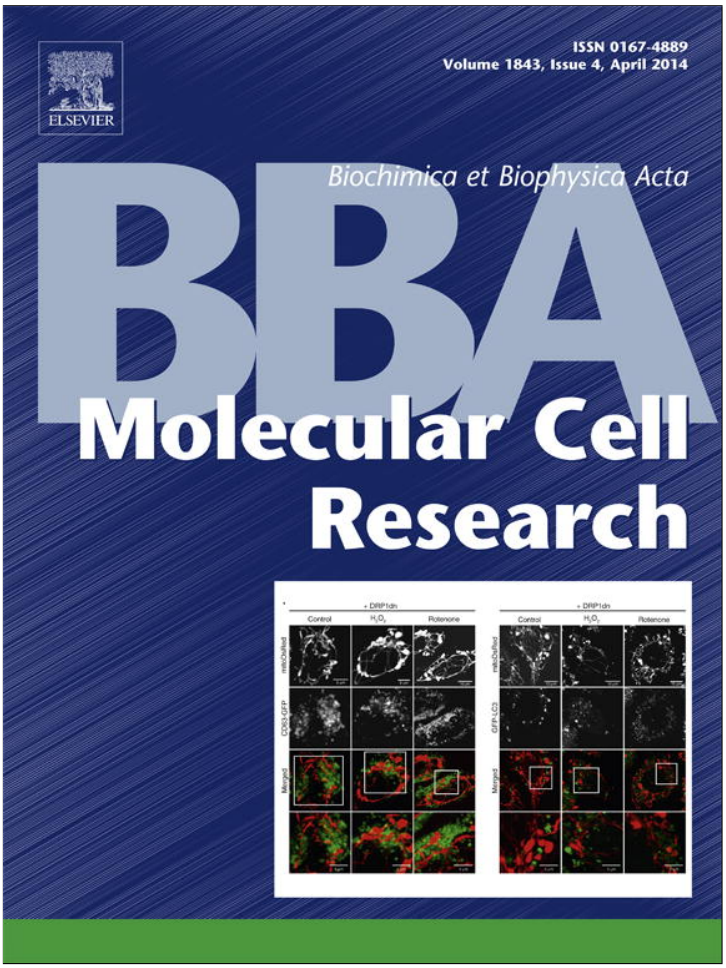

Biochimica et Biophysica Acta 1843 (2014) 769–779

Contents lists available at ScienceDirect

Biochimica et Biophysica Acta

journal homepage: www.elsevier.com/locate/bbamcr

Emerging role for RNA binding motif protein 4 in the development of brown adipocytes

Jung-Chun Lin [a,*], Woan-Yuh Tarn [b], Wen-Kou Hsieh [b]

[a] School of Medical Laboratory Science and Biotechnology, College of Medical Science and Technology, Taipei Medical University, Taipei, Taiwan
[b] Institute of Biomedical Sciences, Academia Sinica, Taipei, Taiwan

ARTICLE INFO

Article history:
Received 19 May 2013
Received in revised form 21 December 2013
Accepted 24 December 2013
Available online 2 January 2014

Keywords:
Alternative splicing
BMP7
Brown adipocyte
Insulin receptor
RBM4

ABSTRACT

RNA-binding motif protein 4 (RBM4) reportedly reprograms the tissue-specific splicing network which modulates the development of muscles and pancreatic β-islets. Herein, we report that *Rbm4a*$^{-/-}$ mice exhibited hyperlipidemia accompanied with reduced mass of interscapular brown adipose tissue (iBAT). Elevated RBM4a led to the isoform shift of *IR*, *Ppar-γ*, and *Pref-1* genes which play pivotal roles in the different stages of adipogenesis. Overexpression of RBM4a enhanced the mitochondrial activity of brown adipocyte-like lineage in the presence of uncoupling agent. RBM4a-ablated adipocytes inversely exhibited impaired development and inefficient energy expenditure. Intriguingly, overexpressed RBM4a induced the expression of brown adipocyte-specific factors (*Prdm16* and *Bmp7*) in white adipocyte-like lineage, which suggested the potential action of RBM4a on the white-to-brown *trans*-differentiation of adipocytes. In differentiating adipocytes, RBM4a constituted a feed-forward circuit through autoregulating the splicing pattern of its own transcript. Based on these results, we propose the emerging role of RBM4 in regulating the adipocyte-specific splicing events and transcription cascade, which subsequently facilitate the development and function of brown adipocyte-like cells.

1. Introduction

Alternative splicing is an important mechanism for regulating gene expression and expanding proteomic diversity in eukaryotes [1–3]. The meticulous expression of alternatively spliced isoforms is the predominant means of controlling cell types and functional specification that consequently influences organogenesis. Exon usage is modulated by the complex interplay between *trans*-acting factors and *cis*-elements within the alternatively spliced pre-messenger RNA [4]. Over 90% of human genes have been demonstrated to undergo at least one alternative splicing event [5,6], but further investigation is required to decipher the detailed mechanisms involved. Moreover, comprehensive insights into alternative splicing are indispensable for understanding the origins of genomic defects.

RNA-binding motif protein 4 (RBM4) is a multifunctional protein that participates in regulating alternative splicing and mRNA translation [7–11]. We previously reported that RBM4 modulates the utilization of alternative exons within several genes which encode muscle and pancreas-specific isoforms [7,10]. RBM4 synergizes its effect on muscle-specific splicing network by inducing the exon 11-skipped isoform of polypyrimidine tract-binding protein (PTB), a myogenic repressor, which is eliminated by nonsense-mediated mRNA decay during myogenesis [10]. A study with *Rbm4* knockout mice shows that RBM4 also facilitates the development of pancreatic islets [11]. The notable augmentation of pancreas-specific factors, such as Ngn3 and Pdx1, upon RBM4 overexpression suggests its influence in promoting pancreas development. RBM4 overexpression also induces the alternatively spliced isoforms of Pax4 and Isl1 which have more-prominent effect on activating the transcription of *insulin* gene in β-islets. Taken together, RBM4 modulates splicing events which in turn influence organogenesis.

Unbalanced energy homeostasis has led to a substantial rise in worldwide incidences of obesity and other metabolic diseases. Obesity is principally caused by accumulation of white adipose tissue (WAT), the cells of which contain a unilocular fat droplet and few mitochondria [12]. In contrast, brown adipose tissue (BAT) is comprised of multilocular lipid droplets and abundant mitochondria. The relatively high metabolic activity of BAT suggests its therapeutic potential for combating obesity and metabolic diseases [13]. The canonical BAT shares a developmental origin with the skeletal muscle, but presumably not with WAT [14]. Classical brown adipocytes arise from *Myf5*-positive progenitors during the prenatal development and subsequently populate interscapular BAT [15,16]. However, so-called beige/brite cells are occasionally found as abundant clusters in WAT of adult animals which are exposed to a cold environment. These inducible adipocytes are derived from *Myf5*-negative lineages, but have both morphological and biological features of classical brown adipocytes [17]. A recent study indicated that platelet-derived growth factor (PDGF) α receptor-positive progenitor cells isolated from WAT develop into BAT-like cells upon β-adrenergic

* Corresponding author at: School of Medical Laboratory Science and Biotechnology, Taipei Medical University, 250, Wu-Hsing Street, Taipei 11031, Taiwan. Tel.: +886 2 27361661x3330; fax: +886 2 27324510.
E-mail address: lin2511@tmu.edu.tw (J.-C. Lin).

0167-4889/$ – see front matter © 2013 Elsevier B.V. All rights reserved.
http://dx.doi.org/10.1016/j.bbamcr.2013.12.018

agonist treatment [18]. Interest is emerging to pursue the mechanism involved in the development of brite cells in terms of fat metabolism.

Adipogenesis is regulated by a complex network involving various hormones and growth factors [19], of which the insulin signaling plays a pivotal role in the development of both white and brown adipocytes [20]. Insulin receptor (IR) substrates act as the docking molecules for the corresponding hormones which in turn activate downstream signaling pathways [21]. Among them, bone morphogenetic proteins (BMPs) substantially contribute to the development of distinct adipose tissues [22]. BMP2 and BMP4 are majorly critical for the commitment step and complete development of WAT [23–25]. On the other hand, BMP7 has been shown to trigger the development of brown adipocytes from both committed and uncommitted precursors [26]. BMP7 activates the expression of PRDM16, the master regulator of BAT development, which represses the formation of WAT and the skeletal muscle [15,26]. Moreover, BMP7 promotes the activation of p38 mitogen-activated protein kinase (MAPK) pathway which is essential for mitochondrial biogenesis in developing BAT [27]. *Bmp7* knockout mice inversely exhibit significant paucity of interscapular BAT during embryonic development. Besides transcription cascade, alternative splicing constitutes another molecular mechanism which modulates adipocyte development. The alternative-spliced transcript of Peroxisome proliferator-activated receptor gamma (*Ppar-γ*) encodes the adipocyte-specific isoform, PPAR-γ2, which is the predominant activator of adipose development [28]. By contrast, the repressive effect of preadipocyte factor 1 (Pref-1) on adipocyte development is relieved in the relatively high expression of alternatively spliced isoforms, *Pref-1C* and *Pref-1D* [29].

Our work constitutes the first demonstration of autoregulated alternative splicing which mediates the increase in RBM4a during adipogenesis. Upregulation of RBM4a subsequently reprograms the adipocyte-specific alternative splicing events which exhibit enormous influence on promoting adipocyte development *in vitro*. The upregulated BAT-related factors in RBM4-overexpressed preadipocytes and the relative paucity of interscapular BAT in *Rbm4a*$^{-/-}$ mice both substantiates that RBM4a could be contributive to the development of BAT.

2. Material and methods

2.1. Serum biochemistry and mice dissection

Male *RBM4a*$^{-/-}$ mice were generated as previously described [11]. After 8 weeks of feeding a regular diet, mice had access to food and water for 1 h at the beginning of the dark phase and then were starved for 8 h. Serum triglyceride (TG) was measured on a Fuji Dri-Chem Clinical Chemistry Analyzer FDC 3500 (housed at the Taiwan Mouse Clinic, Taipei, Taiwan). After a mouse was euthanized, interscapular fat tissues were collected, weighed, and immediately frozen at −80 °C until the RNA and proteins were extracted.

2.2. Cell culture and differentiation

Primary preadipocytes were isolated from the interscapular WAT and BAT of *RBM4a*$^{-/-}$ mice and its wild-type littermates. In brief, the dissected adipose tissues were soaked in HEPES buffer containing type I collagenase and incubated at 37 °C with gentle shaking for 30 min. After being filtered through a 25 μm pore-size nylon filter, the dissociated cells were collected and cultured in a 12-well plate with pre-warm DMEM supplemented with 10% (vol/vol) newborn calf serum, 2.4 nM insulin, 25 μg/ml sodium ascorbate and 10 mM HEPES. The plated cells were washed with fresh medium the next day and replenished culture medium every second day. Mouse NIH3T3 and C2H10T1/2 cells were cultured in DMEM (Invitrogen) supplemented with 10% fetal bovine serum (FBS) (Invitrogen). To induce adipogenesis, primary adipocytes were cultured in the medium supplemented with 5 μM dexamethasone, 0.02 μM insulin, 0.5 mM isobutylmethylxanthine, 1 nM T3, 125 μM indomethacin, and 1 μM rosiglitazone. Forty-eight hours after induction, cells were cultured in DMEM supplemented with 0.02 μM insulin and 1 nM T3 which mediated the differentiation of primary adipocytes. Differentiation of NIH3T3 and C3H10T1/2 cells was conducted by culturing the cells in induction medium supplemented with 20% FBS, 0.5 mM IBMX, 12.7 μM dexamethasone, and 10 μg/ml insulin. Forty-eight hours after induction, the induction medium was replaced with differentiation medium (DM) supplemented with 10% FBS and 10 μg/ml insulin and replenished every 2 days.

2.3. Plasmid construction, transfection and RT-PCR analysis

Expression vectors for mouse RBM4a isoforms were constructed by placing the coding sequence in-frame into pCDNA3.1-FLAG (Invitrogen). Expressing vectors containing a mutated RNA recognition motif or zinc knuckle domain of RBM4a were constructed using the QuikChange site-directed mutagenesis system (Stratagene). The ph*Rbm4a* minigene reporter was constructed by sequential insertion of two human *Rbm4a* genomic fragments into the pCH110 vector (Amersham Pharmacia). The *Rbm4a* fragments were as follows: 3738-bp exon 2–intron 2 (nucleotides 66407183–66410920) and 2617-bp exon 3–exon 4 (66410921–66413537; NM_002896). NIH3T3 and C3H10T1/2 cells were grown to 50%–60% confluence and transfected using PolyJet (SignaGen) with the indicated plasmid. After 24 h, total RNA was extracted using the TRIzol reagent (Invitrogen). For RT-PCR assay, 2 μg of RNA was reverse-transcribed by SuperScriptase III (Invitrogen) in a 10-μl reaction. The PCR analysis of individual genes was performed in 30 (*Gapdh*) or 35 thermal cycles (other genes) with gene-specific primer sets (see Table S1). A quantitative RT-PCR was performed with SYBR green fluorescent dye and gene-specific primer sets (see Table S2) using an ABI One Step™ PCR machine (Applied Biosystems). The relative mRNA level was quantitated by the ΔΔ−Ct method, and the level of *Gapdh* mRNA served as the internal control.

2.4. Immunoblotting and subcellular fractionation

Immunoblotting of cell lysates or tissue extracts was performed using an enhanced chemiluminescence system (PerkinElmer). Images were analyzed by the LAS-4000 imaging system (Fujifilm). The primary antibodies applied in this study included polyclonal antibodies against RBM4 [7], insulin receptor (Santa Cruz), lamin (Santa Cruz), and p38 MAPK (Cell Signaling), and monoclonal antibodies against the FLAG epitope (M2, Sigma-Aldrich), tubulin (Thermo Fisher Scientific), and phosphorylated p38 MAPK (Cell Signaling Technology). For a subcellular fractionation analysis, cells were resuspended in 500 ml of RSB-100 (10 mM Tris–HCl, 100 mM NaCl, and 2.5 mM $MgCl_2$; pH 7.4) containing 40 mg/ml digitonin (Calbiochem). After incubation on ice for 5 min, cells were centrifuged at 2000 *g* for 8 min. The supernatant was collected as the cytosolic fraction, and the pellet was resuspended in 500 ml of RSB-100 containing 0.5% Triton X-100 for a further 5-min incubation on ice. After centrifugation at 2000 *g* for 8 min, the supernatant was collected as the nuclear fraction.

2.5. Immunofluorescence

Indirect immunofluorescence was performed as described previously [30]. Primary antibodies used in this study were polyclonal antibodies against RBM4 and monoclonal antibodies against the FLAG epitope (20 μg/ml; Sigma). Secondary antibodies were used as described previously [7]. Images were observed using the TE2000-U microscopy system (Nikon).

2.6. Oil-Red-O staining

Proliferating and differentiating cells were washed twice with phosphate-buffered saline (PBS) and fixed with 4% paraformaldehyde for 60 min at room temperature. Cells were washed with PBS twice

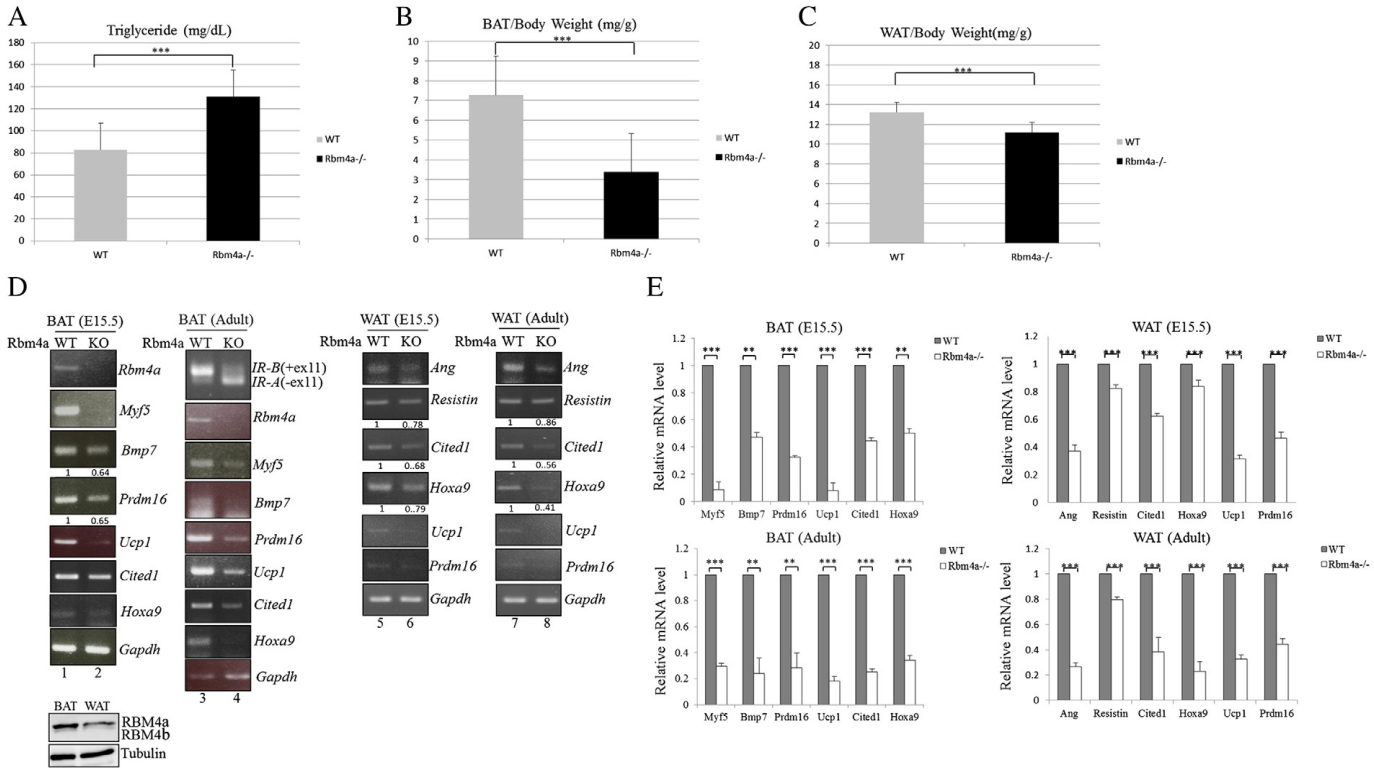

Fig. 1. *Rbm4a*$^{-/-}$ mice exhibit hyperlipidemia and impaired brown adipose tissue (BAT) development. Eight-week old wild-type (WT) and *Rbm4a*$^{-/-}$ male mice were subjected to the following examinations. (A) Serum triglyceride of fasting mice is quantified (WT, 82.83 mg/dl ± 11.3 mg/dl, $n = 6$; *Rbm4a*$^{-/-}$, 131 ± 19.12 mg/dl, $n = 6$; ***, $p < 0.005$). (B) Interscapular BAT isolated from WT and *Rbm4a*$^{-/-}$ mice were weighted and normalized to the body weight ($n = 6$; ***, $p < 0.005$). (C) Interscapular white adipose tissue (WAT) isolated from mice were weighted and normalized to the body weight ($n = 6$; ***, $p < 0.005$). (D) Total RNA isolated from the iBAT and iWAT was subjected to RT-PCR using specific primer sets (see Table S1). Total lysates of isolated BAT and WAT were subjected to immunoblotting analysis using indicated antibodies. (E) mRNA level of each factor in interscapular brown and white adipose tissues was quantified by quantitative RT-PCR (qRT-PCR) using specific primer sets (right panel; see Table S2). Glyceraldehyde 3 phosphate dehydrogenase (*Gapdh*) mRNA served as a loading control.

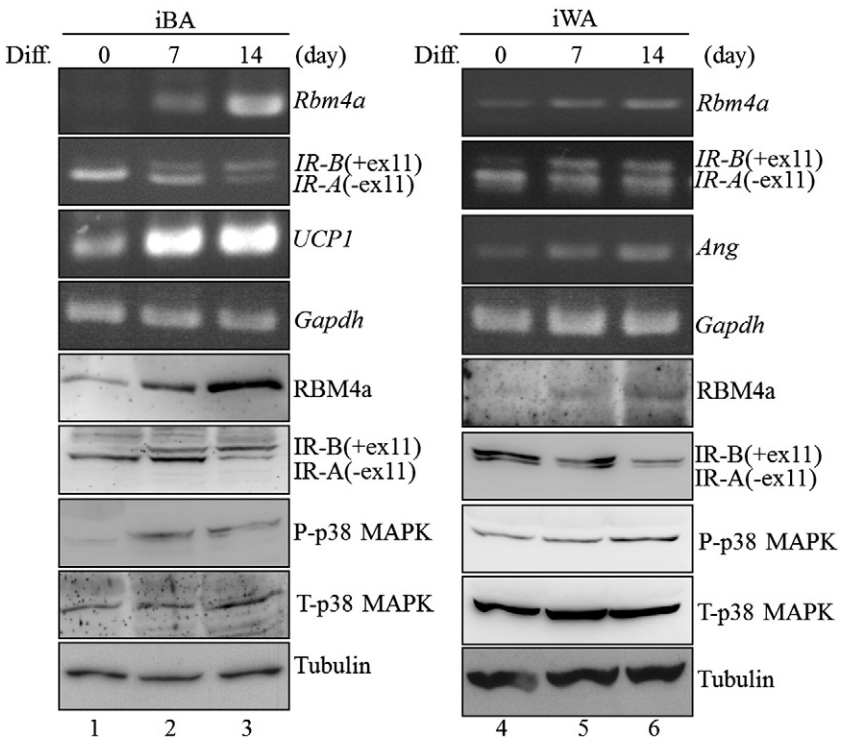

Fig. 2. Expression of RBM4a and adipocyte-related factors in differentiating adipocyte. Primary interscapular brown and white adipocytes (iBA and iWA) were cultured in differentiation medium (DM) for 7 and 14 days. Total RNA was isolated and then subjected to RT-PCR analysis with specific primer sets (see Table S1). *Gapdh* served as a loading control. Cell lysates were fractionated on separate gels, followed by immunoblotting with the indicated antibodies.

and rinsed with 60% isopropanol for 5 min at room temperature. Equilibrated cells were stained with a 0.3% filtered Oil-Red-O solution (Sigma) for 10 min at room temperature. Stained cells were washed with distilled water for 3 times. For extraction of Oil-Red-O dye, the culture dish with absolute isopropanol was shaken at room temperature for 2 h. The extract was centrifuged and analyzed at 550 nm using a NanoDrop 2000 spectrophotometer (Thermo).

2.7. Mitochondria respiration assay

A Seahorse XF24 extracellular flux analyzer (Seahorse Bioscience, North Billerica, MA, USA) was used to measure the oxygen consumption rate (OCR; as an indicator of mitochondrial respiration). In brief, 50,000 preadipocytes or C3H10T1/2 cells were seeded in each well of Seahorse XF24 plates with 150 μl of DMEM and incubated overnight. Prior to the measurement, cells were washed with unbuffered media and immersed in 675 μl unbuffered media without CO_2 for 1 h. The OCR was assessed in 8-min cycles as recommended by Seahorse Bioscience. The basal OCR level was recorded first, and following injection of FCCP, the maximal OCR was revealed.

3. Results

3.1. *Rbm4a*$^{-/-}$ mice exhibit hyperlipidemia and impaired BAT development

In mice, there are two copies of the *Rbm4* gene (namely *Rbm4a* and *Rbm4b*) adjacent to each other on the same chromosome [11]. *Rbm4a*$^{-/-}$ mice exhibited defective production of insulin, which resulted in significant hyperglycemia [11]. The close relation between hyperglycemia and hyperlipidemia prompted the investigation into the impact of high glucose on TG metabolism in *Rbm4a*$^{-/-}$ mice [31]. Biochemical analysis showed that starved wild-type mice exhibited normal level of serum TG (Fig. 1A, 82.83 mg/dl [$n = 6$]), whereas the elevated TG level was examined in *Rbm4a*$^{-/-}$ mice (131 mg/dl [$n = 6$]). In addition, high glucose was considered as the adipogenic inducer [32] and we therefore examined the impact of hyperglycemia on the development of adipose tissue in *Rbm4a*$^{-/-}$ mice. About 50% reduction in the interscapular BAT (iBAT) mass and 15% reduction in the interscapular WAT (iWAT) mass was noted in *Rbm4a*$^{-/-}$ adult mice as compared to the wild-type littermates (Fig. 1B and C).

The relatively prominent expression of RBM4a over RBM4b in iBAT as compared with iWAT once again implied the influence of RBM4a on BAT development (Fig. 1D, lower panel and Fig. S1). We next asked whether depletion of RBM4a affected the development of BAT. As shown by RT-PCR analysis, ablation of *Rbm4a* increased the level of exon 11-skipped *insulin receptor* (*IR*) isoform in adult iBAT (Fig. 1D, lane 4) as was shown in *Rbm4a*-depleted muscle and pancreatic cells [10,11]. The impaired expression of BAT-specific markers (*Myf5*, *Bmp7*, *Prdm16* and *Ucp1*) was also noted in the *Rbm4a*$^{-/-}$ BAT (Fig. 1D, lanes 2 and 4). A growing body of evidence has demonstrated the action of Myf5 on committing myoblastic lineages including the skeletal muscle and brown adipocytes [15,16]. In addition, upregulated BMP7 and PRDM16 were also shown to commit the complete development of brown adipocytes [26]. The results indicated the defective development of *Rbm4a*-depleted iBAT in the prenatal and postnatal stages. On the other hand, the reduced level of WAT-specific markers (*Angiotensinogen*, *Resistin*) and brite cell markers (*Cited1* and *Hoxa9*) in *Rbm4a*$^{-/-}$ iWAT suggested the potential effect of RBM4a on WAT development and white-to-brown *trans*-differentiation of adipocytes (Fig. 1D, lanes 6 and 8). The expression profile of adipocyte-related genes in *Rbm4a*$^{-/-}$ adipose tissues and their counterparts was further quantified using Quantitative RT-PCR (qRT-PCR, Fig. 1E). These results showed the wide impact of RBM4a ablation on the development of distinct adipocytes.

3.2. Expression of RBM4a and adipocyte-related factors during adipogenesis

We next wondered whether the expression of RBM4a protein was modulated during adipocyte differentiation. Increase in the BAT-specific *Ucp1* (Fig. 2, lanes 2 and 3) and WAT-specific *Ang* transcript

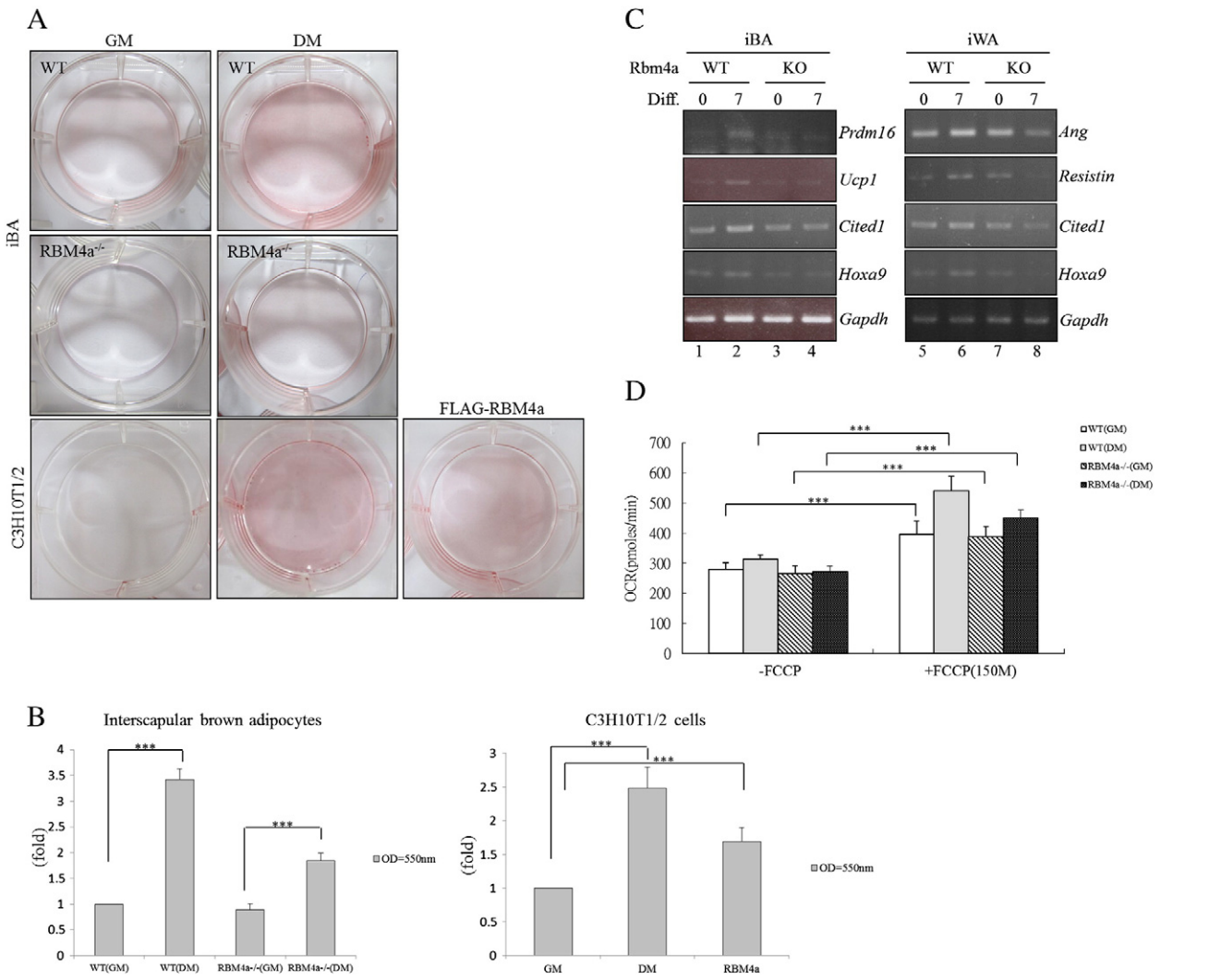

Fig. 3. Ablation of RBM4a impairs the adipocyte differentiation. (A) Primary preadipocytes isolated from the iBAT of wild-type and *Rbm4a*$^{-/-}$ mice were cultured in growth medium (GM) or DM for 7 days. The mock vector-transfected C3H10T1/2 cells were cultured in GM or DM for 7 days; the FLAG-RBM4a vector-transfected cells were cultured in GM and then subjected to the Oil-Red-O staining. (B) The bar graph showed the spectrophotometric analysis of Oil-Red-O optical density (OD) at 550 nm after being extracted from the stained cells in previous experiments (*, $p < 0.05$; **, $p < 0.01$; ***, $p < 0.005$). (C) The RNA was extracted from WT and *Rbm4a*$^{-/-}$ preadipocytes (iBA/iWA) cultured in GM or DM for 7 days and subjected to the RT-PCR analysis using specific primer sets. (D) Graphs presented the oxygen consumption rate (OCR) of proliferation and differentiation WT and *Rbm4a*$^{-/-}$ iBA toward FCCP treatment. Values shown were the mean ± SEM of three individual experiments for each group (***, $p < 0.005$).

(lanes 5 and 6) manifested the effective differentiation of interscapular brown and white adipocytes (iBA and iWA) [33,34]. RT-PCR and immunoblotting assay showed a gradual increase in *Rbm4a* transcript and protein which resulted in the upregulated *IR-B* isoform in differentiating primary adipocytes. The gradual increase in IR-B subsequently induced the hyperphosphorylation of p38 MAPK which was essential to the development of brown adipocytes rather than white adipocytes [11,19,35]. The results showed that RBM4a could act as an effector in adipogenesis-required signaling pathway.

3.3. *RBM4a*$^{-/-}$ preadipocytes exhibit impaired differentiation

The primary adipocytes isolated from *RBM4a*$^{-/-}$ iBAT and wild type iBAT were established to evaluate the influence of RBM4a on adipogenesis. Oil-Red-O staining showed that less lipid droplet were noted in differentiating *RBM4a*$^{-/-}$ iBA (Fig. 3A, middle, DM) as compared with its wild-type littermates (Fig. 3A, upper, DM). Inversely, RBM4a-overexpressed C3H10T1/2 cells exhibited the lipid droplet accumulation as was seen in differentiating cells (Fig. 3A, lower). The effect of differentiation condition and RBM4a overexpression on adipogenesis was quantitatively evaluated in terms of the extracted Oil-Red-O using spectrophotometric analysis (Fig. 3B). *Rbm4a*$^{-/-}$ adipocytes exhibited insignificant induction of adipocyte-specific markers toward differentiation condition, which indicated its impaired differentiation (Fig. 3C, lanes 4 and 8). Besides the cell differentiation, the downregulated *Ucp1* suggested the altered energetics in the *RBM4a*$^{-/-}$ adipocytes. The reserve capacity of mitochondria was measured in the presence of the electron transport uncoupler FCCP (0.5 μM) to verify this hypothesis. No significant difference in the basic respiratory rate was noted between the proliferating wild-type and *RBM4a*$^{-/-}$ brown adipocytes (Fig. 3D, white and downward bar). Nevertheless, the oxygen consumption rate of differentiating *RBM4a*$^{-/-}$ iBA was lower (black bar) than those of wild-type iBA (gray bar) in the presence of FCCP, which suggested the impaired energy expenditure in *RBM4a*$^{-/-}$ adipocytes. The results suggested that ablation of RBM4a abolished not only the development but also the physiological function of brown adipocytes.

3.4. RBM4a enhances adipocyte differentiation

The shift in the alternative splicing of *Pref-1* gene was demonstrated to relieve its repressive effect on adipogenesis and in turn commit the pre-adipocytes to terminal differentiation [29]. The significant shift in

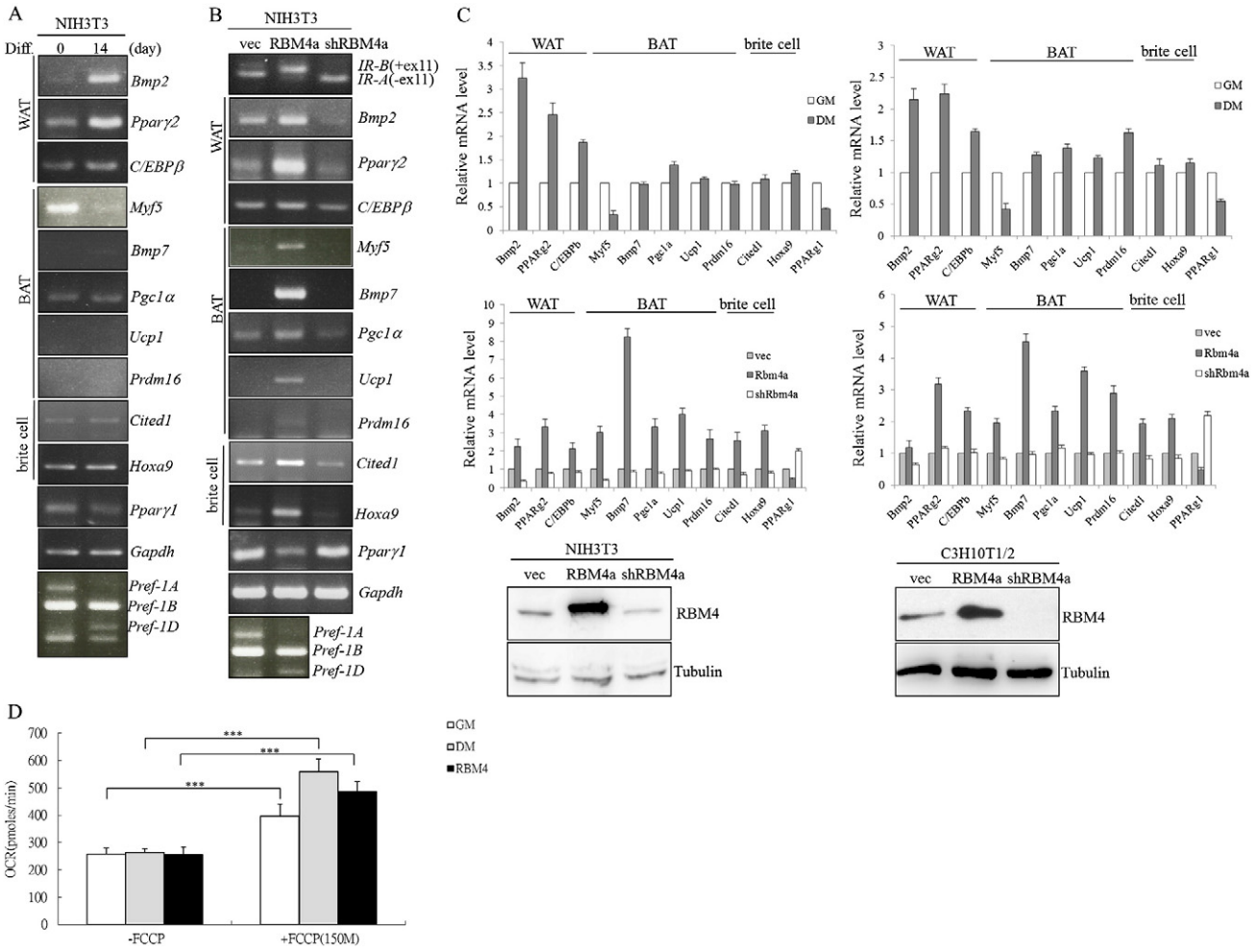

Fig. 4. RBM4a promotes the adipocytic transcription network. (A) NIH3T3 cells were cultured in GM or DM for 14 days. Total RNA was extracted and subjected to RT-PCR using specific primer pairs as indicated. (B) NIH3T3 cells were transiently transfected with the mock vector, or the FLAG-RBM4a-expressing vector or the RBM4a-targeting shRNA expressing vector and cultured in GM for 24 h. RT-PCR analysis was performed as described for panel A. (C) mRNA level of each factor in NIH3T3 (left three panels) and C3H10T1/2 cells (right three panels) cultured under the indicated conditions was quantified by qRT-PCR using specific primer set (see Table S2). The bar graph showed the results from three independent experiments. Total cell lysate isolated from NIH3T3 and C3H10T1/2 cells was subjected to immunoblotting assay using indicated antibodies. (D) Graphs presented the oxygen consumption rate of proliferation, differentiation and RBM4a overexpressing C3H10T1/2 cells toward FCCP treatment. Values shown were the mean ± SEM of three individual experiments for each group (***, $p < 0.005$).

Pref-1A/B to *Pref-1D* was noted in the differentiating (Fig. 4A) and RBM4-overexpressed NIH3T3 cells (Fig. 4B) which exhibited upregulated WAT-specific markers, whereas the knockdown of endogenous RBM4a led to the expression of adipocyte-specific factors (Fig. 4B, shRBM4a). The presence of overexpressed RBM4a also resulted in the decrease in *Ppar-γ1* concomitant with an increased level of *Ppar-γ2*, which represented another adipocyte-specific splicing event (Fig. 4A and B). The parallel experiments were conducted with the BAT-like lineage, C3H10T1/2 cells [26,36] to specifically evaluate the effect of RBM4a on brown adipocytes. The similar trend to the expression of adipocyte-specific markers was showed in the RBM4a-overexpressed C3H10T1/2 as was seen in NIH3T3cells (Fig. 4C, lower panel). However, the significant response of BAT-specific factors were only noted in the differentiating C3H10T1/2 cells (Fig. 4C, upper panel, BAT), but not the NIH3T3 cells. Besides the upregulation of adipocyte-specific factors, the RBM4a-overexpressed C3H10T1/2 cells exhibited the elevated oxygen consumption rate toward FCCP treatment, which illustrated the influence of RBM4a on the function of BAT (Fig. 4D, RBM4). These results revealed the effect of RBM4a overexpression on enhancing the differentiation and function of BAT-like lineage, which echoed to the impaired development of *Rbm4a*$^{-/-}$ interscapular BAT (Figs. 1D and 3D).

3.5. RBM4a autoregulates its expression by directing alternative splicing

The increase in RBM4a protein has been noted during the differentiation of distinct cells [10,11], the mechanism involved in this regulation has not been addressed. Notably, a search of the NCBI EST database revealed an alternatively-spliced isoform of *Rbm4a* in small rodents. We wondered whether the isoform shift in *Rbm4a* transcript participated in the regulation of its protein level. The endogenous *Rbm4a* isoforms were amplified using the PCR primers which specifically targeted the conserved exon 2 and the 3′ untranslated region (UTR) of the *Rbm4a* transcript (Fig. 5A). The relatively high level of full-length transcript (Fig. 5B, upper panel) corresponded with the quantity of RBM4a protein in the skeletal muscle, testis and kidney (Fig. 5B, lower panel, lanes 2, 3 and 6). By contrast, the exon 3-skipped isoform (*Rbm4a-iso2*) was predominantly expressed in the liver, placenta, bone marrow and adrenal gland, of which the RBM4a protein was nearly absent (Fig. 5B, lanes 4, 5, 7 and 8). Nevertheless, the lower amount of canonical *Rbm4a* transcript concomitant with a relatively high level of RBM4a protein in the heart implied that additional post-transcriptional event may participate in regulating RBM4a expression. The *Rbm4a* full-length transcript was also elevated in differentiating cells, which corresponded with the increase in RBM4a protein (Fig. 5C).

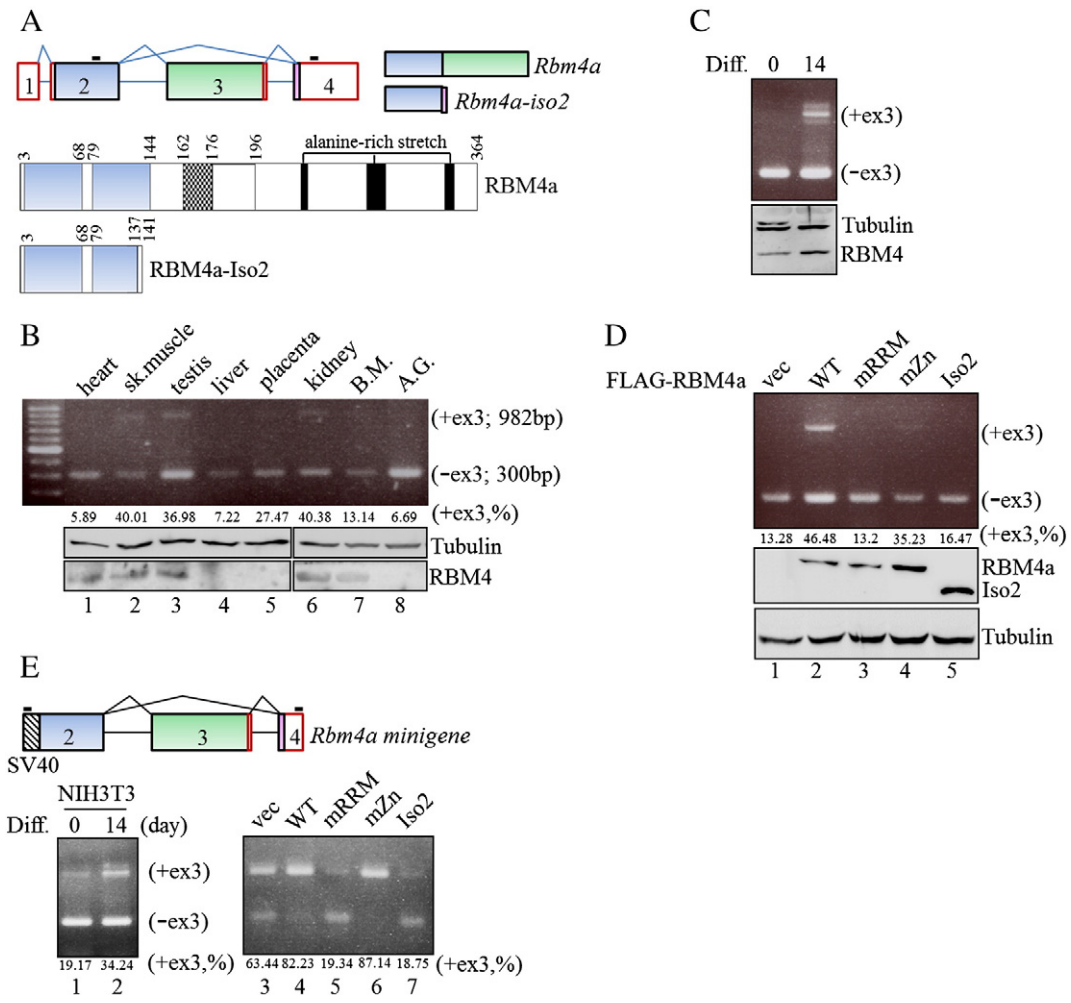

Fig. 5. *Rbm4a* transcripts are alternatively spliced. (A) The diagrams show two mouse *Rbm4a* isoforms that were identified with specific primer set. Schematic representation indicates the domains of mouse RBM4a isoforms. (B) Total RNA and the tissue extract were isolated from different mouse tissues and subjected to RT-PCR and immunoblotting analysis using a specific primer set and antibody against *Rbm4a*. The values given below the bands represent relative levels of the full length *Rbm4a* isoform over all *Rbm4a* transcripts. (C) Total RNA and cell lysate isolated from proliferation or differentiation NIH3T3 cells were subjected to RT-PCR and immunoblotting analysis using a specific primer set and antibody against *Rbm4a*. (D) NIH3T3 cells were transiently transfected with the mock vector or vector expressing wild-type or various RBM4a mutants. The overexpressed-protein level and splicing profile of *Rbm4a* isoforms were analyzed as described for panel A. Values given below the bands represented relative mRNA level of full length *Rbm4a* transcript. (E) Diagram illustrates the *Rbm4a* minigene construct and the checkered box represents the SV40 promoter. The pCH-hRbm4a minigene was cotransfected with RBM4a-expressing vectors in NIH3T3 cells. The splicing products were analyzed by RT-PCR using primer set as shown in Table S1.

To investigate whether RBM4a modulated the splicing of its own transcript, the splicing pattern of endogenous *Rbm4a* transcript was analyzed with the reverse primer targeting the 3′UTR which is absent from the RBM4a expression vector. The full-length *Rbm4a* transcript was markedly elevated in the presence of exogenous wild-type RBM4a (Fig. 5D, lane 2) but not RBM4a-Iso2 or other engineered mutants (lanes 3–5). The Rbm4a minigene vector, pCH-Rbm4a, which contained the complete genomic segment from exon 2 to the 3′UTR was next constructed to verify the effect of RBM4a on the splicing of its own transcript (Fig. 5E, upper panel). RT-PCR analysis showed the significant increase in the full-length *Rbm4a* analog in the presence of differentiation medium, wild-type FLAG-RBM4a and the zinc knuckle mutant (Fig. 5E, lanes 2, 4 and 6). On the contrary, the exon 3-skipped isoform was noted in the presence of mutated RRM-harboring RBM4a and RBM4a-Iso2 (lanes 5 and 7). An analogous result also showed the loss of the canonical *Rbm4a* transcript in the *Rbm4b*$^{-/-}$ BAT (Fig. S2). These results suggested that the canonical RBM4a constituted a feedforward circuit which autoregulated the selection of exon 3 within its own transcript.

3.6. RBM4a-Iso2 antagonizes the autoregulatory mechanism

The ubiquitously high level of *Rbm4a-iso2* isoform prompted the following investigation into its effect on the expression of full-length RBM4a. As shown in Fig. 6, the presence of exogenous RBM4a-Iso2 abolished the exon 3 inclusion of endogenous *Rbm4a* in a dose-dependent manner (Fig. 6B, left panel), which resulted in the reduced level of endogenous RBM4a protein (Fig. 6A). Moreover, the exogenous RBM4a-Iso2 antagonized the effect of canonical RBM4a with regard to the isoform shift in *IR* and *Ppar-γ* genes and the upregulation of adipocyte-specific factors (Fig. 6B, right panel; Fig. 6C).

Majority of endogenous RBM4a was shown to distribute in the nucleus of proliferating NIH3T3 cells (Fig. 6D, upper panel, GM), but translocated to the cytoplasm of differentiating cells (Fig. 6D, upper panel, DM). On the contrary, exogenous RBM4-Iso2 not only showed the steady distribution in the cytoplasm of proliferating and differentiating cells (Fig. 6D, upper panel, FLAG-Iso2), but also directed the cytoplasmic localization of endogenous RBM4a protein in proliferating cells (Fig. 6D, right panel). Subcellular fractionation showed the similar

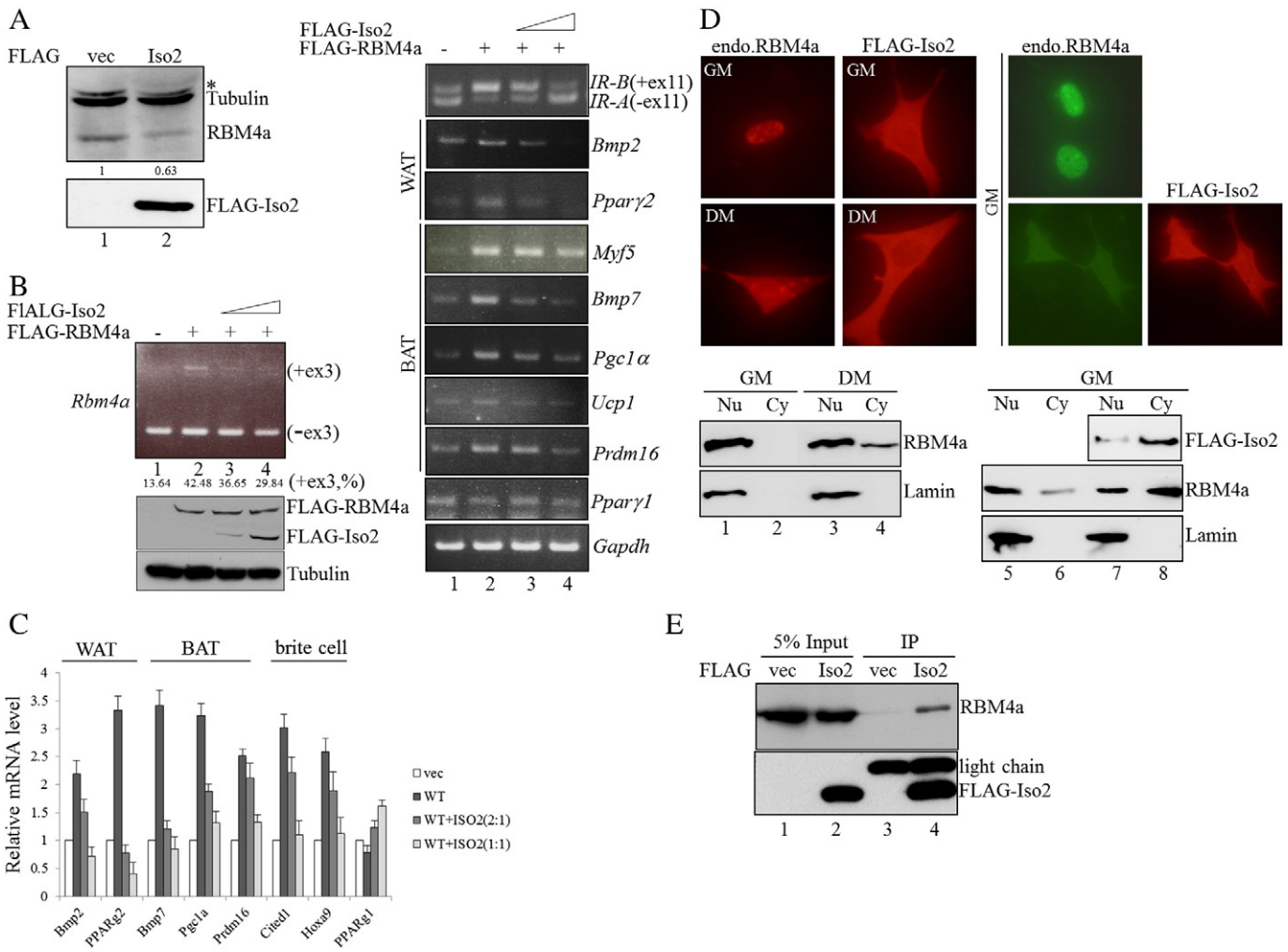

Fig. 6. Expression of RBM4a is autoregulated via alternative splicing. (A) NIH3T3 cells were transfected with the mock vector or the vector expressing FLAG-RBM4 isoform 2 (Iso2). Immunoblotting was performed on the same membranes (separated by a blank space) using indicated antibodies. (B) The FLAG-RBM4a expression vector was transfected alone (lane 2) or with increasing amounts of the FLAG-RBM4a Iso2 expression vector (lanes 3 and 4) to NIH3T3 cells. Splicing profile of *Rbm4a* and the level of adipose-related factors were assayed by RT-PCR as previously described. FLAG-tagged proteins were examined by immunoblotting with anti-FLAG antibody. (C) mRNA level of adipose-related factors in parallel experiments was quantified using qRT-PCR with specific primer sets as previously described. (D) The mock vector or FLAG-RBM4a Iso2-overexpressed NIH3T3 cells were cultured in growth medium (GM) or differentiation medium (DM) for 7 days and then subjected to immunofluorescence assay using indicated antibodies. The lower panel showed the subcellular distribution of endogenous RBM4a and the FLAG-tagged Iso2 variant (right) in proliferating or differentiating NIH3T3 cells using anti-RBM4 or anti-FLAG antibody; Lamin was used as a loading control. (E) Total cell extracts were prepared from mock vector or FLAG-RBM4a Iso2-transfected NIH3T3 cells grown in GM and subjected to anti-FLAG immunoprecipitation followed by immunoblotting assay.

results that the nucleus RBM4a translocated to the cytoplasm of differentiating and RBM4a-Iso2 overexpressed cells (Fig. 6D; lower panel, lanes 4 and 8). The colocalized distribution of RBM4a isoforms in proliferating cells (Fig. 6D, right) and the result of immunoprecipitation analysis demonstrated the association between RBM4a isoforms *in vivo* (Fig. 6E, lane 4). These results suggested that the interplay between RBM4a isoforms could disturb the cellular distribution of canonical RBM4a, which in turn fine-tuned its effect on splicing regulation.

3.7. RBM4a regulates adipogenesis through multiple mechanisms

RBM4a has been demonstrated to affect the expression of multiple pancreas-specific factors in a alternative splicing-mediated regulation [11] or through uncertain mechanism. Nevertheless, the existence in RBM4a of a zinc knuckle (CCHC) motif implied the putative action of RBM4a on transcriptional regulation. RT-PCR analysis showed that the mutant and deletion of RNA recognition motif abolished the effect of RBM4a on the splicing of *IR* and *Ppar-γ* and induced expression of *Bmp2*, *Pgc1α* and *Ucp1* (Fig. 7A, mRRM and Iso2). By contrast, the mutant and absence of zinc knuckle motif largely impaired the influence of RBM4a on *Bmp7* and *Prdm16* expression (Fig. 7A, mZn and Iso2). Conspicuously, the expression of *Myf5* showed no response only to the presence RBM4a-Iso2 in preadipocytes. The influence of exogenous RBM4 proteins on the expression profile of adipocyte-specific factors differed from the biological activity, but not the expression level in transfected cells (Fig. 5D, lower panel). qRT-PCR assay showed the similar trend to the expression of adipocyte-specific markers as was noted using RT-PCR analysis (Fig. 7B). These results suggested that RBM4a may modulate the expression of adipocyte-related factors through posttranscriptional regulation and transcriptional control.

4. Discussion

Classical brown adipocytes are demonstrated to originate from *Myf5*-positive progenitors in the prenatal stage [15,16] whereas the beige/brite cells arise from *Myf5*-negative lineage in response to cold stress or PPARγ agonists in the postnatal stage [17]. Nevertheless, the mechanism involved in the development of beige/brite cells is still poorly understood. Drastic elimination of *Myf5* in the embryonic *Rbm4a*$^{-/-}$ BAT rather than adult BAT (Fig. 1D, lanes 2 and 4) suggested its critical

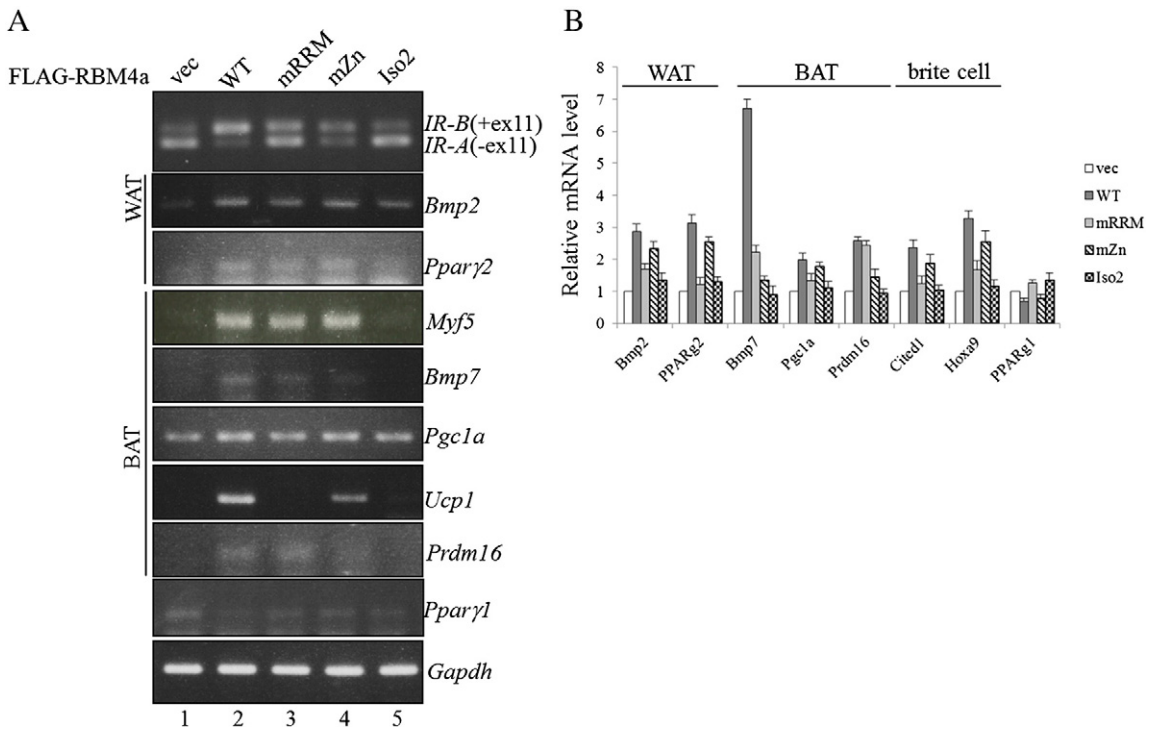

Fig. 7. RBM4a modulates BAT development through distinct mechanisms. (A) NIH3T3 cells were transiently transfected with the mock vector or the expression vectors encode various RBM4a proteins. Splicing profile of *IR* and the level of adipose-related factors were assayed by RT-PCR as previously described. (B) mRNA level of adipose-related factors in parallel experiment was quantified using qRT-PCR with specific primer sets.

role in the development of myoblastic lineage. The low respiratory rate of *Rbm4a*$^{-/-}$ iBA indicated the action of RBM4a on the physiological function of iBA. The diminished *Cited1* and *Hoxa9* expression in adult *Rbm4a*$^{-/-}$ adipose tissues rather than embryonic adipocytes (Fig. 1D, lanes 4 and 8) implied the influence of RBM4a on the white-to-brown *trans*-differentiation of adipocytes. This speculation was initially proved with the upregulation of the BAT-specific markers in the WAT-like lineage which expressed exogenous RBM4a (Fig. 4B). On the other hand, the action of RBM4a on white adipocyte-specific factors still suggested its potential effect on the development of WAT-like lineage, which echoed to the reduced iWAT mass in *Rbm4a*$^{-/-}$ mice. The significant influence of RBM4a on the classical brown adipocytes and brite cells may explain why *Rbm4a*$^{-/-}$ mice exhibited a trifling reduction in WAT concomitant with a significant loss in BAT mass.

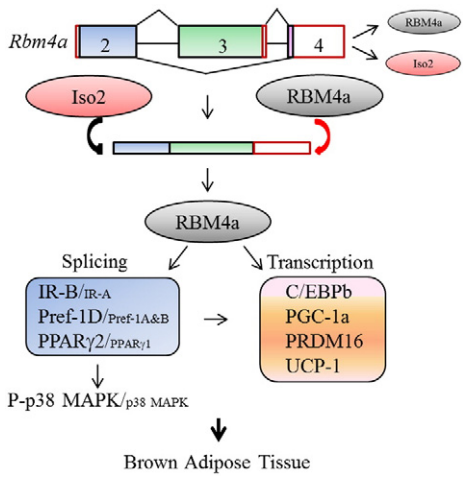

Fig. 8. RBM4a modulated the splicing profile of *IR*, *Pref-1*, *Ppar-γ* and its own transcript during adipogenesis. RBM4a expression was autoregulated through the alternative splicing mechanism. Inhibition of adipocyte differentiation was relieved in the presence of RBM4a-increased *Pref-1D* isoform. RBM4-induced PPARγ2 in turn activated the adipocyte-specific transcription network. The increase in RBM4a induced IR-B expression, subsequently activating the downstream p38 MAPK signaling which was required for the development of BAT.

Continuous studies illustrated how splicing factors reprogrammed the splicing profile which determined the cell fate and function. For instance, two *Nova* genes were demonstrated to regulate more than 700 neuron-specific splicing events [37]. CELF family members regulated the muscle-specific splicing network which greatly influenced myocyte development and function [38]. RBM4 was demonstrated to promote the complete development of the skeletal muscle and pancreatic islets by means of reprogramming the tissue-specific splicing network [10,11]. *IR* gene is alternatively spliced to encode the exon 11-excluded IR-A and exon 11-included IR-B isoforms [39]. An increase in IR-A expression activated insulin growth factor (IGF) signaling which largely contributed to the proliferation of preadipocytes in the prenatal stage, whereas upregulated IR-B isoform activated insulin signaling which directed the development of adult adipocytes [40]. A marked shift from isoform IR-A to IR-B has been noted during the differentiation of progenitors to brown adipocytes [33]. However, supplementation with either IR isoform failed to commit the differentiation of *IR*-ablated brown preadipocytes [33]. Furthermore, excess IR expression was associated with an inability to undergo adipogenesis [33], implying that elevated IR abundance may impair the IGF-IR signaling by competing with downstream signaling pathways [41]. These results indicated that the meticulous modulation of *IR* isoforms played a pivotal role in adipocyte differentiation. The CTG-expanded dmpk transcript mediated the nuclear accumulation of CUG-binding protein 1 and hnRNP H protein, which in turn antagonized the effect of muscleblind 1 protein on promoting IR-B production in the skeletal muscles of patients with myotonic dystrophy type 1 [42–46]. These results illustrated that the splicing of IR pre-mRNA was regulated by the balance between various splicing factors, which severely influenced the fate and function of specific cells. In this study, RBM4 was demonstrated to increased the

relative level of IR-B which is required for complete differentiation of brown adipocytes.

Alternative splicing was considered as a regulatory mechanism in fine-tuning the activity of transcriptional factors. Pref-1 served as a dominant repressor at the onset of adipocyte differentiation [47]. The repressive effect of Pref-1 on adipogenesis was attenuated through both transcriptional regulation [48] and alternative splicing events [29]. In this study, RBM4a was demonstrated as the first splicing factor which reprogrammed the splicing pattern of *Pref-1* (Fig. 4B). On the other hand, the ubiquitously expressed PPAR-γ1 was reported to enhance the development of adipocytes embedded in the liver, whereas PPAR-γ2 specifically regulated the development of interscapular adipose tissues [49,50]. RBM4 was revealed as the first splicing regulator which modulated the isoform shift of *Ppar-γ* during adipogenesis. These results indicated that RBM4 could reprogram the adipocyte-specific splicing network which in turn regulated adipocyte development.

The spatiotemporal balance between various splicing factors determined the splicing profile in particular cell types and developmental stages. Hence, the expression of splicing factors must be meticulously controlled. Negative autoregulation was demonstrated to be an effective mechanism for maintaining the precise level of many splicing factors. For example, Tra-2 SR proteins, including SRp20, SC35 and ASF, autoregulated the splicing patterns of their respective transcripts [51–54]. The expression of mammalian PTB and SC35 protein was negatively autoregulated by producing premature termination codon-containing pre-mRNA which was subsequently degraded by the nonsense-mediated decay pathway [54,55]. Excess SRp20 directed a negative-control mechanism by favoring the expression of an exon 4-skipping SRp20 isoform [51]. In this study, the increase in canonical RBM4a established a feed-forward circuit by increasing the relative ratio of its canonical isoform. However, upregulated RBM4a may interfere with the interaction between its transcript and other splicing factor, such as PTB which served as the antagonizer to the RBM4a-regulated splicing event [10]. Nevertheless, the isoform shift of RBM4a transcripts sheds new light on a positive-control mechanism by which the expression of RBM4a was manipulated.

In conclusion, our results showed that RBM4a promoted the development of brown adipocytes by integrating the splicing regulation and transcriptional control in distinct stages of adipogenesis (Fig. 8). Moreover, the feed-forward mechanism was first constituted, which contributed to the autoregulation of RBM4a in differentiating adipocytes. We propose that the effect of RBM4a on the development and function of BAT may suggest its therapeutic potential for combating metabolic diseases and obesity.

Acknowledgements

We greatly appreciate Prof. Yueh-Hsing Ou (National Yang-Ming University, Taiwan) for providing C3H10T1/2 cells. This work was supported by Taipei Medical University grant TMU100-AE1-B17. We declare that no conflicts of interest exist.

Appendix A. Supplementary data

Supplementary data to this article can be found online at http://dx.doi.org/10.1016/j.bbamcr.2013.12.018.

References

[1] D.L. Black, Mechanisms of alternative pre-messenger RNA splicing, Annu. Rev. Biochem. 72 (2003) 291–336.
[2] B.J. Blencowe, Alternative splicing: new insights from global analyses, Cell 126 (2006) 37–47.
[3] T.W. Nilsen, B.R. Graveley, Expansion of the eukaryotic proteome by alternative splicing, Nature 463 (2010) 457–463.
[4] M. Chen, J.L. Manley, Mechanisms of alternative splicing regulation: insights from molecular and genomics approaches, Nat. Rev. Mol. Cell Biol. 10 (2009) 741–754.
[5] Q. Pan, O. Shai, L.J. Lee, B.J. Frey, B.J. Blencowe, Deep surveying of alternative splicing complexity in the human transcriptome by high-throughput sequencing, Nat. Genet. 40 (2008) 1413–1415.
[6] E.T. Wang, R. Sandberg, S. Luo, et al., Alternative isoform regulation in human tissue transcriptomes, Nature 456 (2008) 470–476.
[7] J.C. Lin, W.Y. Tarn, Exon selection in alpha-tropomyosin mRNA is regulated by the antagonistic action of RBM4 and PTB, Mol. Cell. Biol. 25 (2005) 10111–10121.
[8] J.C. Lin, M. Hsu, W.Y. Tarn, Cell stress modulates the function of splicing regulatory protein RBM4 in translation control, Proc. Natl. Acad. Sci. U. S. A. 104 (2007) 2235–2240.
[9] J.C. Lin, W.Y. Tarn, RNA-binding motif protein 4 translocates to cytoplasmic granules and suppresses translation via argonaute2 during muscle cell differentiation, J. Biol. Chem. 284 (2009) 34658–34665.
[10] J.C. Lin, W.Y. Tarn, RBM4 down-regulates PTB and antagonizes its activity in muscle cell-specific alternative splicing, J. Cell Biol. 193 (2011) 509–520.
[11] J.C. Lin, W.Y. Tarn, W.K. Hsieh, et al., RBM4 promotes pancreas cell differentiation and insulin expression, Mol. Cell. Biol. 33 (2013) 319–327.
[12] K.W. Park, D.S. Halperin, P. Tontonoz, Before they were fat: adipocyte progenitors, Cell Metab. 8 (2008) 454–457.
[13] A. Bartelt, J. Heeren, The holy grail of metabolic disease: brown adipose tissue, Curr. Opin. Lipidol. 23 (2012) 190–195.
[14] S. Cinti, The adipose organ, Prostaglandins Leukot. Essent. Fat. Acids 73 (2005) 9–15.
[15] P. Seale, B. Bjork, W. Yang, et al., PRDM16 controls a brown fat/skeletal muscle switch, Nature 454 (2008) 961–967.
[16] P. Seale, S. Kajimura, B.M. Spiegelman, Transcriptional control of brown adipocyte development and physiological function-of mice and men, Genes Dev. 23 (2009) 788–797.
[17] A. Frontini, S. Cinti, Distribution and development of brown adipocytes in the murine and human adipose organ, Cell Metab. 11 (2010) 253–256.
[18] Y.H. Lee, A.P. Petkova, E.P. Mottillo, et al., In vivo identification of bipotential adipocyte progenitors recruited by beta3-adrenoceptor activation and high-fat feeding, Cell Metab. 15 (2012) 480–491.
[19] S. Gesta, Y.H. Tseng, C.R. Kahn, Developmental origin of fat: tracking obesity to its source, Cell 131 (2007) 242–256.
[20] E.D. Rosen, O.A. MacDougald, Adipocyte differentiation from the inside out, Nat. Rev. Mol. Cell Biol. 7 (2006) 885–896.
[21] M.F. White, The IRS-signalling system: a network of docking proteins that mediate insulin action, Mol. Cell. Biochem. 182 (1998) 3–11.
[22] T.J. Schulz, Y.H. Tseng, Emerging role of bone morphogenetic proteins in adipogenesis and energy metabolism, Cytokine Growth Factor Rev. 20 (2009) 523–531.
[23] R.R. Bowers, J.W. Kim, T.C. Otto, et al., Stable stem cell commitment to the adipocyte lineage by inhibition of DNA methylation: role of the BMP-4 gene, Proc. Natl. Acad. Sci. U. S. A. 103 (2006) 13022–13027.
[24] R.R. Bowers, M.D. Lane, A role for bone morphogenetic protein-4 in adipocyte development, Cell Cycle 6 (2007) 385–389.
[25] W. Jin, T. Takagi, S.N. Kanesashi, et al., Schnurri-2 controls BMP-dependent adipogenesis via interaction with Smad proteins, Dev. Cell 10 (2006) 461–471.
[26] Y.H. Tseng, E. Kokkotou, T.J. Schulz, et al., New role of bone morphogenetic protein 7 in brown adipogenesis and energy expenditure, Nature 454 (2008) 1000–1004.
[27] J. Lu, S.Y. Xu, Q.G. Zhang, et al., Bupivacaine induces apoptosis via mitochondria and p38 MAPK dependent pathways, Eur. J. Pharmacol. 657 (2011) 51–58.
[28] E. Mueller, S. Drori, A. Aiyer, et al., Genetic analysis of adipogenesis through peroxisome proliferator-activated receptor gamma isoforms, J. Biol. Chem. 277 (2002) 41925–41930.
[29] B. Mei, L. Zhao, L. Chen, et al., Only the large soluble form of preadipocyte factor-1 (Pref-1), but not the small soluble and membrane forms, inhibits adipocyte differentiation: role of alternative splicing, Biochem. J. 364 (2002) 137–144.
[30] M.C. Lai, H.W. Kuo, W.C. Chang, et al., A novel splicing regulator shares a nuclear import pathway with SR proteins, EMBO J. 22 (2003) 1359–1369.
[31] E.D. Rosen, B.M. Spiegelman, Adipocytes as regulators of energy balance and glucose homeostasis, Nature 444 (2006) 847–853.
[32] A. Paola, L. Sara, Z. Barbara, et al., High glucose induces adipogenic differentiation of muscle-derived stem cells, Proc. Natl. Acad. Sci. U. S. A. 105 (2008) 1226–1231.
[33] A.J. Entingh, C.M. Taniguchi, C.R. Kahn, Bi-directional regulation of brown fat adipogenesis by the insulin receptor, J. Biol. Chem. 278 (2003) 33377–33383.
[34] E.M. Lindgren, R. Nielsen, N. Petrovic, et al., Noradrenaline represses PPAR (peroxisome-proliferator-activated receptor) gamma2 gene expression in brown adipocytes: intracellular signalling and effects on PPARgamma2 and PPARgamma1 protein levels, Biochem. J. 382 (2004) 597–606.
[35] J.A. Engelman, M.P. Lisanti, P.E. Scherer, Specific inhibitors of p38 mitogen-activated protein kinase block 3T3-L1 adipogenesis, J. Biol. Chem. 273 (1998) 32111–32120.
[36] J. Klein, M. Fasshauer, H.H. Klein, et al., Novel adipocyte lines from brown fat: a model system for the study of differentiation, energy metabolism, and insulin action, Bioessays 24 (2002) 382–388.
[37] C. Zhang, M.A. Frias, A. Mele, et al., Source Integrative modeling defines the Nova splicing-regulatory network and its combinatorial controls, Science 329 (2010) 439–443.
[38] J.C. Castle, C. Zhang, J.K. Shah, et al., Expression of 24,426 human alternative splicing events and predicted cis regulation in 48 tissues and cell lines, Nat. Genet. 40 (2008) 1416–1425.
[39] A. Ullrich, J.R. Bell, E.Y. Chen, et al., Human insulin receptor and its relationship to the tyrosine kinase family of oncogenes, Nature 313 (1985) 756–761.
[40] J. Giudice, F.C. Leskow, D.J. Arndt-Jovin, et al., Differential endocytosis and signaling dynamics of insulin receptor variants IR-A and IR-B, J. Cell Sci. 124 (2011) 801–811.

[41] D. Maggi, C. Laurino, G. Andraghetti, et al., The overexpression of insulin receptor makes CHO cells resistant to the action of IGF-1: role of IRS-1, Biochem. Biophys. Res. Commun. 205 (1994) 693–699.
[42] M. Fardaei, M.T. Rogers, H.M. Thorpe, et al., Three proteins, MBNL, MBLL and MBXL, co-localize in vivo with nuclear foci of expanded-repeat transcripts in DM1 and DM2 cells, Hum. Mol. Genet. 11 (2002) 805–814.
[43] A.N. Ladd, N. Charlet, T.A. Cooper, The CELF family of RNA binding proteins is implicated in cell-specific and developmentally regulated alternative splicing, Mol. Cell. Biol. 21 (2001) 1285–1296.
[44] J.W. Miller, C.R. Urbinati, P. Teng-Umnuay, et al., Recruitment of human muscleblind proteins to (CUG) (n) expansions associated with myotonic dystrophy, EMBO J. 19 (2000) 4439–4448.
[45] S. Paul, W. Dansithong, D. Kim, et al., Interaction of muscleblind, CUG-BP1 and hnRNP H proteins in DM1-associated aberrant IR splicing, EMBO J. 25 (2006) 4271–4283.
[46] L.T. Timchenko, RNA CUG repeats sequester CUGBP1 and alter protein levels and activity of CUGBP1, J. Biol. Chem. 276 (2001) 7820–7826.
[47] M. Rakhshandehroo, A. Koppen, E. Kalkhoven, Pref-1 preferentially inhibits heat production in brown adipose tissue, Biochem. J. 443 (2012) e3–e5.
[48] J. Armengol, J.A. Villena, E. Hondares, et al., Pref-1 in brown adipose tissue: specific involvement in brown adipocyte differentiation and regulatory role of C/EBPδ, Biochem. J. 443 (2012) 799–810.
[49] S. McClelland, R. Shrivastava, J.D. Medh, Regulation of translational efficiency by disparate 5′ UTRs of PPARgamma splice variants, PPAR Res. (2009) 193413.
[50] L. Wang, S. Xu, J.E. Lee, et al., Histone H3K9 methyltransferase G9a represses PPARγ expression and adipogenesis, EMBO J. 32 (2013) 45–59.
[51] H. Jumaa, P.J. Nielsen, The splicing factor SRp20 modifies splicing of its own mRNA and ASF/SF2 antagonizes this regulation, EMBO J. 16 (1997) 5077–5085.
[52] W. Mattox, B.S. Baker, Autoregulation of the splicing of transcripts from thetransformer-2 gene of *Drosophila*, Genes Dev. 5 (1991) 786–796.
[53] S. Sun, Z. Zhang, R. Sinha, et al., SF2/ASF autoregulation involves multiple layers of post-transcriptional and translational control, Nat. Struct. Mol. Biol. 17 (2010) 306–312.
[54] A. Sureau, R. Gattoni, Y. Dooghe, et al., SC35 autoregulates its expression by promoting splicing events that destabilize its mRNAs, EMBO J. 20 (2001) 1785–1796.
[55] M.C. Wollerton, C. Gooding, E.J. Wagner, et al., Autoregulation of polypyrimidine tract binding protein by alternative splicing leading to nonsense-mediated decay, Mol. Cell 13 (2004) 91–100.